

# Magnetic Characterization of Nanowire Arrays Using First Order Reversal Curves

R. Lavín<sup>1</sup>, J. C. Denardin<sup>1</sup>, J. Escrig<sup>1</sup>, D. Altbir<sup>1</sup>, A. Cortés<sup>2</sup>, and H. Gómez<sup>3</sup>

<sup>1</sup>Departamento de Física, Universidad de Santiago de Chile, Santiago 917-0124, Chile

<sup>2</sup>Departamento de Física, Universidad Técnica Federico Santa María, Valparaíso 2390123, Chile

<sup>3</sup>Instituto de Química, Universidad Católica de Valparaíso, Casilla 4059 Valparaíso, Chile

Arrays of Ni nanowires have been studied by means of first order reversal curves (FORC) diagrams. The dependence of the coercivity of the arrays as a function of the length of the nanowires has been experimentally investigated. We have shown that the FORC diagrams provide detailed information about the distribution of interactions and coercivities and allowed us to observe the reversible component of magnetization. Our results are in good agreement with analytical calculations obtained by means of a simple model.

**Index Terms**—First order reversal curves (FORC), magnetic nanowires.

## I. INTRODUCTION

THE study of highly ordered arrays of magnetic wires is a topic of growing interest. The high ordering, together with the magnetic nature of the wires, may give rise to outstanding cooperative properties of fundamental and technological interest [1]–[3]. In these arrays, inter-element interactions play an important role and have been subject to strong investigation [4]–[6].

For the study of these systems, different techniques have been used. For the structural characterization usually scanning electron microscopy (SEM) and atomic/magnetic force microscopy (AFM/MFM) has been used. The magnetic characterization is usually made by measuring hysteresis curves. However it is not possible to obtain information of interactions and coercivity distributions from these measurements. Then, and within this context, the first order reversal curves (FORC) diagrams appear as a useful tool for the characterization of magnetic systems [7]–[11]. The FORC diagrams of these arrays allow us to get also an insight on the relative proportions of reversible and irreversible components of the magnetization which are important for technological devices. In this work we investigate the FORC diagrams of three arrays of Ni nanowires which lead us to obtain important information of the magnetic behavior of the arrays as a function of the length of the nanowires.

## II. EXPERIMENTAL SETUP

Three hexagonal arrays of Ni nanowires of diameters  $d = 2R = 50$  nm and lengths  $L = 1, 4$  and  $12$   $\mu\text{m}$  have been prepared by electrodeposition into nanopores of alumina membranes with interpore distance  $D = 100$  nm [12], [13]. The electrodeposition was performed at a constant potential (dc electrodeposition at  $-1.0$  v). The morphology of the individual nanowires after the dissolution of the alumina was studied by means of scanning electron microscopy (SEM) with a JEOL

5900 LV and transmission electron microscopy (TEM) using a JEOL 2010 F, checking the high ordering of the hexagonal arrays and their large aspect ratio [6].

The chemical characterization of the nanowires was made by means of energy-dispersive analysis of x-rays (EDAX), obtaining a clear peak corresponding to the emission spectrum of Ni. The magnetization measurements were performed with a home-made alternating gradient force magnetometer (AGFM), with the applied field parallel to the axis of nanowires, and at ambient temperature. The samples contain  $\sim 10^9$  Ni nanowires each.

## III. RESULTS AND DISCUSSION

Fig. 1 illustrates the hysteresis curves for the three arrays of nanowires as a function of the length  $L$  of the nanowires. In this figure a strong increase of the coercivity and remanence with the length  $L$  is evidenced. These measurements lead us to obtain the coercivity of the three samples, as illustrated with dots in Fig. 2. In order to understand the dependence of the coercivity on the length, we developed analytical calculations using a simple model. We considered that each nanowire is along the  $z$  axis and reverse its magnetization from one of its minima,  $M = M_0\hat{z}$  to the other,  $M = -M_0\hat{z}$  by means of the propagation of a transversal wall [14]. To calculate the coercivity of an isolated wire we used an adapted Stoner-Wohlfarth model in which the length of the particle which experienced a coherent rotation is replaced by the length of the domain wall. We also included the effect of dipolar interactions of the array, which lowers the energy barriers for the switching. The interaction field was calculated using the expression developed by Laroze *et al.* [15] for the interaction energy of two nanowires a distance  $D$  apart

$$\begin{aligned}\tilde{E}_{\text{int}}(D) &\equiv \frac{E_{\text{int}}(D)}{V} \\ &= \frac{\mu_0 M_0^2 R^2}{2LD} \left( 1 - \frac{1}{\sqrt{1 + \frac{L^2}{D^2}}} \right).\end{aligned}$$

To compare with our experimental results we calculated the non-dimensional magnetostatic interaction energy

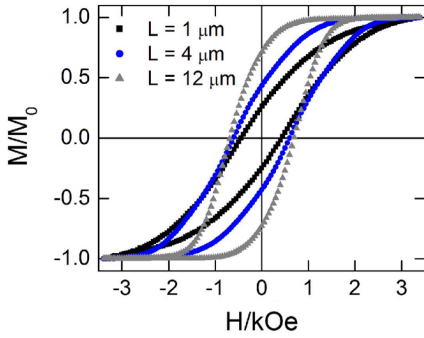


Fig. 1. Hysteresis curves for samples with lengths  $L = 1, 4,$  and  $12 \mu\text{m}$ , inter-pore distance  $D = 100 \text{ nm}$ , and diameter  $d = 2R = 50 \text{ nm}$ , produced under the same chemical conditions. The external magnetic field was applied parallel to the axis of nanowires.

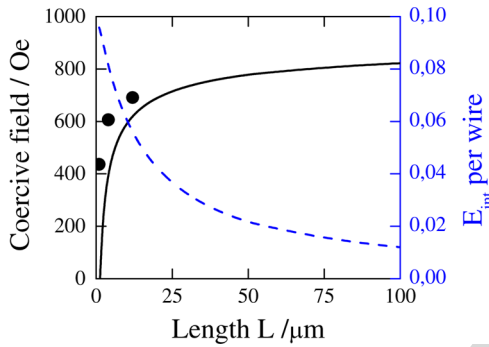


Fig. 2. (Solid line) coercivity calculated for an array of nanowires with  $d = 2R = 50 \text{ nm}$ , and  $D = 100 \text{ nm}$ . (Black dots) experimental values obtained from Fig. 1, and (dash line) the non-dimensional magnetostatic interaction energy per wire as a function of the length  $L$ .

per wire by adding all the contributions in the array,  $\sum_{i=1}^{N-1} \sum_{j=i+1}^N (\dot{E}_{\text{int}}(D)/\mu_0 M_0^2 N)$ , with  $N$  the number of nanowires in the array. Due to present computational capabilities we considered  $N = 70000$ . This energy is illustrated in Fig. 2 with a dashed line. Using these results and following calculations in [6] we obtain the coercivity as a function of the length of the array, which is also depicted with a solid line in Fig. 2. In this figure a good agreement between experimental and analytical results is observed. As a result of the decrease of the interaction energy with the increasing length of the wires in the array, the coercivity decreases approaching the result for the non interacting case ( $E_{\text{int}} = 0$ ). It is also expected a decrease of the interaction field with increasing  $L$  because of the relation between the interaction energy and field.

The measurement of a FORC starts by saturating the sample at a large positive applied field. Then the field is decreased to a reversal field,  $H_a$ . The FORC is defined as the magnetization curve that results when the applied field is increased from  $H_a$  back to saturation. The magnetization at the applied field  $H_b$  on the FORC with reversal point  $H_a$  is denoted by  $M(H_a, H_b)$ , where  $H_b \geq H_a$ .

A statistical model that describes the system as a set of bistable entities (hysteron) based on the Preisach model [7], [16] is used to illustrate and obtain information from the FORC. The

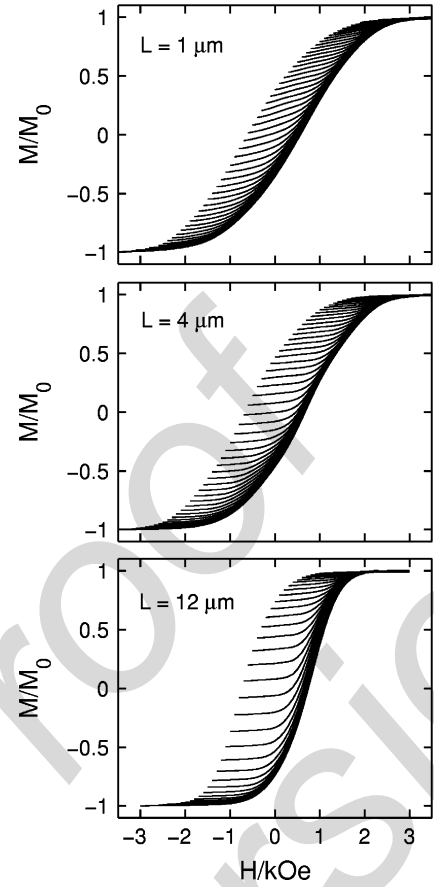


Fig. 3. First order reversal curves (FORC) for samples with different lengths. The external magnetic field was applied parallel to the nanowire axis. Each FORC have been measured with external field intervals of  $100 \text{ Oe}$  between points.

extended probability density function (pdf) of the ensemble is defined by [9], [17]

$$\rho(H_a, H_b) = -\frac{1}{2} \frac{\partial^2 M}{\partial H_a \partial H_b}. \quad (1)$$

This function extends over the entire plane  $H_a, H_b$ . A FORC diagram is a contour plot of the pdf (1), and can be presented in terms of the variables  $H_c = (H_b - H_a)/2$  and  $H_i = (H_b + H_a)/2$  which are the fields of switching (coercivity of hysteron) and interaction (bias of each hysteron) [9], allowing to capture the reversible component of the magnetization, which appears focused on  $H_c = 0$ . The pdf (1) of a sample is obtained by numerical derivation of  $M(H_a, H_b)$ , which contains all FORC measurements. The FORC diagram is obtained performing the contour plot of the pdf (1).

Fig. 3 illustrates the FORCs obtained for the three arrays investigated and Fig. 4 depicts the corresponding contour plots of the pdf (1), i.e., the FORC diagrams of the samples.

In the FORC diagrams of the samples (Fig. 4) a very large distribution of the interaction fields (in the  $H_i$  direction) is observed, which is expected for highly interacting systems. One can also observe from the diagrams that as  $L$  increase the distribution of interaction decrease. This result is in agreement with our analytical results presented in Fig. 2 (dash line) where a

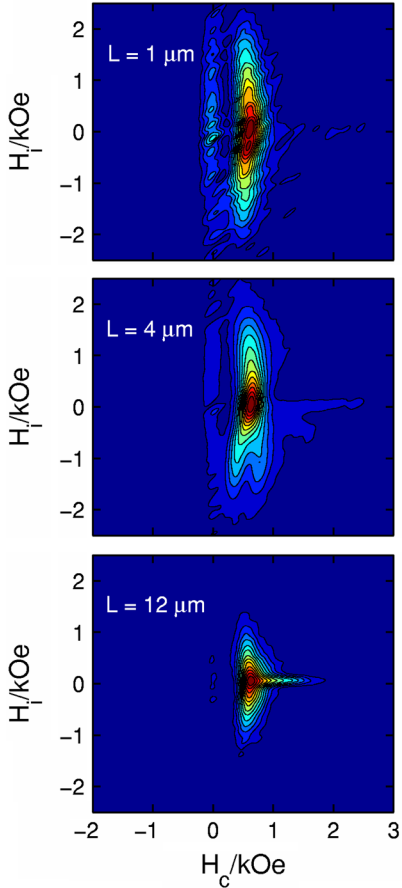


Fig. 4. The FORC diagrams for the three samples studied. These FORC diagrams were obtained performing the contour plots of the pdf (1), and changing to variables  $H_c$  (coercive field) and  $H_i$  (interaction field), according to the text.

strong decrease of the interaction energy by increasing  $L$  is shown. Since the interaction energy is proportional to the interaction field, the decrease of the distribution of the interaction fields when the length of the wires increase, observed in the FORC diagrams, follows the same tendency of the dashed line in Fig. 2.

Fig. 5 depicts the distribution of coercivities at the interaction field  $H_i = 0$ , i.e.,  $\rho(H_c, H_i = 0)/\rho_0$ . In this figure it is shown that by increasing  $L$  the coercivity distribution slightly enhances and the field at which the maximum occur is shifted to higher values. This last feature of the coercivity distribution is in agreement with the behavior of the measured coercivity, which increases for longer nanowires, as shown in Fig. 2. The maximum of the coercive distribution for the three samples are at  $H_c = 574$  Oe,  $H_c = 600$  Oe and  $H_c = 700$  Oe for samples with  $L = 1, 4,$  and  $12 \mu\text{m}$  respectively.

Another important feature which appears in the FORC diagrams is the reversible component of the magnetization. The relative importance of this component, which appears in the FORC diagram at  $H_c = 0$  (Figs. 4 and 5), is not evidenced by measuring the hysteresis curves. This reversible component vanishes as  $L$  increases (Fig. 5), as expected, since a system with

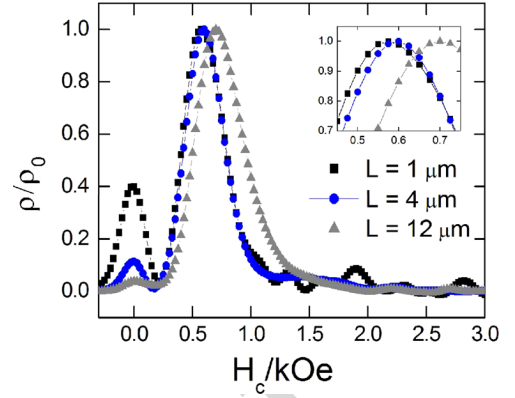


Fig. 5. Distribution of coercivities for the interaction field  $H_i = 0$ , i.e.,  $\rho(H_c, H_i = 0)/\rho_0$ . In the small box it is shown a snapshot of the peaks of the coercivities distribution. At  $H_c = 0$  it is observed a decrease in the reversible component of the magnetization as  $L$  increases.

higher coercivity has a smaller reversible component. Furthermore it is possible to quantify the amount of reversible magnetization of the system as a function of the amount of irreversible magnetization [11], [18].

#### IV. CONCLUSION

The magnetic properties of arrays of Ni nanowires were investigated by means of hysteresis curves and FORC diagrams. Our experimental results were compared with analytical calculations obtained by means of a simple model. The FORC diagrams lead us to obtain a more complete characterization of these systems, giving the coercivity distribution and the reversible and irreversible component of the magnetization, which are difficult to obtain from a simple hysteresis curve. The measured coercivities as a function of the length  $L$  of the wires are in agreement with our analytical results. By increasing the length of the wires in the array an increase of the coercivity and an enhancement of the coercivity distribution are evidenced, as well as a decrease of the reversible component.

#### ACKNOWLEDGMENT

This work was supported in part by the Millennium Science Nucleus *Basic and Applied Magnetism* P06-022F, in part by Fondecyt Grants 11070010, 1080164, and 1080300, and in part by the AFOSR under Contract FA9550-07-1-0040. The CONICYT Ph.D. program and General Direction of Graduates at Universidad de Santiago de Chile (DIGEGRA, USACH) are also acknowledged.

#### REFERENCES

- [1] R. P. Cowburn, D. K. Koltsov, A. O. Adeyeye, M. E. Welland, and D. M. Tricker, "Single-domain circular nanomagnets," *Phys. Rev. Lett.*, vol. 83, pp. 1042–1045, 1999.
- [2] T. Gerrits, H. A. M. van den Berg, J. Hohlfield, L. Bär, and T. Rasing, "Ultrafast precessional magnetization reversal by picosecond magnetic field pulse shaping," *Nature*, vol. 418, pp. 509–512, 2002.

- [3] R. H. Koch, J. G. Deak, D. W. Abraham, P. L. Trouilloud, R. A. Altman, Y. Lu, W. J. Gallagher, R. E. Scheuerlein, K. P. Roche, and S. S. P. Parkin, "Magnetization reversal in micron-sized magnetic thin films," *Phys. Rev. Lett.*, vol. 81, pp. 4512–4515, 1998.
- [4] K. Nielsch, R. B. Wehrspohn, J. Barthel, J. Kirschner, U. Gösele, S. F. Fischer, and H. Kronmüller, "Hexagonally ordered 100 nm period nickel nanowire arrays," *Appl. Phys. Lett.*, vol. 79, pp. 1360–1362, 2001.
- [5] M. Liu, J. Lagdani, H. Imrane, C. Pettiford, J. Lou, S. Yoon, V. G. Harris, C. Vittoria, and N. X. Sun, "Self-assembled magnetic nanowire arrays," *Appl. Phys. Lett.*, vol. 90, no. 103105, 2007.
- [6] J. Escrig, R. Lavín, J. L. Palma, J. C. Denardin, D. Altbir, A. Cortés, and H. Gómez, "Geometry dependence of coercivity in Ni nanowire arrays," *Nanotechnology*, vol. 19, no. 075713, 2008.
- [7] C. R. Pike, A. P. Roberts, and K. L. Verosub, "Characterizing interactions in fine magnetic particle systems using first order reversal curves," *J. Appl. Phys.*, vol. 85, pp. 6660–6667, 1999.
- [8] C. Pike and A. Fernandez, "An investigation of magnetic reversal in submicron-scale Co dots using first order reversal curve diagrams," *J. Appl. Phys.*, vol. 85, pp. 6668–6676, 1999.
- [9] C. R. Pike, "First-order reversal-curve diagrams and reversible magnetization," *Phys. Rev. B*, vol. 68, no. 104424, 2003.
- [10] C. R. Pike, C. A. Ross, R. T. Scalettar, and G. Zimanyi, "First-order reversal curve diagram analysis of a perpendicular nickel nanopillar array," *Phys. Rev. B*, vol. 71, no. 134407, 2005.
- [11] F. Béron, D. Ménard, and A. Yelon, "First-order reversal curve diagrams of magnetic entities with mean interaction field: A physical analysis perspective," *J. Appl. Phys.*, vol. 103, no. 07D908, 2008.
- [12] L. da F. Costa, G. Riveros, H. Gómez, A. Cortés, M. Gilles, E. A. Dalchiele, and R. E. Marotti [Online]. Available: <http://arxiv.org/abs/cond-mat/0504573>
- [13] A. Cortés, G. Riveros, J. L. Palma, J. C. Denardin, R. E. Marotti, E. A. Dalchiele, and H. Gómez, Single-crystal growth of nickel nanowires: influence of deposition conditions on structural and magnetic properties unpublished.
- [14] P. Landeros, S. Allende, J. Escrig, E. Salcedo, D. Altbir, and E. E. Vogel, "Reversal modes in magnetic nanotubes," *Appl. Phys. Lett.*, vol. 90, no. 102501, 2007.
- [15] D. Laroze, J. Escrig, P. Landeros, D. Altbir, M. Vázquez, and P. Vargas, "A detailed analysis of dipolar interactions in arrays of bistable magnetic nanowires," *Nanotechnology*, vol. 18, no. 415708, 2007.
- [16] G. Bertotti, *Hysteresis in Magnetism*. San Diego, CA: Academic Press, 1998.
- [17] L. Spinu, A. Stancu, C. Radu, F. Li, and J. B. Wiley, "Method for magnetic characterization of nanowire structures," *IEEE Trans. Magn.*, vol. 40, pp. 2116–2118, 2004.
- [18] F. Béron, L. Clime, M. Ciureanu, D. Ménard, R. W. Cochrane, and A. Yelon, "Reversible and quasireversible information in first-order reversal curve diagrams," *J. Appl. Phys.*, vol. 101, no. 09J107, 2007.

Manuscript received March 3, 2008. Current version published October 22, 2008. Corresponding author: J. C. Denardin (e-mail: jdenardin@usach.cl).

# Magnetic Characterization of Nanowire Arrays Using First Order Reversal Curves

R. Lavín<sup>1</sup>, J. C. Denardin<sup>1</sup>, J. Escrig<sup>1</sup>, D. Altbir<sup>1</sup>, A. Cortés<sup>2</sup>, and H. Gómez<sup>3</sup>

<sup>1</sup>Departamento de Física, Universidad de Santiago de Chile, Santiago 917-0124, Chile

<sup>2</sup>Departamento de Física, Universidad Técnica Federico Santa María, Valparaíso 2390123, Chile

<sup>3</sup>Instituto de Química, Universidad Católica de Valparaíso, Casilla 4059 Valparaíso, Chile

**Arrays of Ni nanowires have been studied by means of first order reversal curves (FORC) diagrams. The dependence of the coercivity of the arrays as a function of the length of the nanowires has been experimentally investigated. We have shown that the FORC diagrams provide detailed information about the distribution of interactions and coercivities and allowed us to observe the reversible component of magnetization. Our results are in good agreement with analytical calculations obtained by means of a simple model.**

**Index Terms**—First order reversal curves (FORC), magnetic nanowires.

## I. INTRODUCTION

THE study of highly ordered arrays of magnetic wires is a topic of growing interest. The high ordering, together with the magnetic nature of the wires, may give rise to outstanding cooperative properties of fundamental and technological interest [1]–[3]. In these arrays, inter-element interactions play an important role and have been subject to strong investigation [4]–[6].

For the study of these systems, different techniques have been used. For the structural characterization usually scanning electron microscopy (SEM) and atomic/magnetic force microscopy (AFM/MFM) has been used. The magnetic characterization is usually made by measuring hysteresis curves. However it is not possible to obtain information of interactions and coercivity distributions from these measurements. Then, and within this context, the first order reversal curves (FORC) diagrams appear as a useful tool for the characterization of magnetic systems [7]–[11]. The FORC diagrams of these arrays allow us to get also an insight on the relative proportions of reversible and irreversible components of the magnetization which are important for technological devices. In this work we investigate the FORC diagrams of three arrays of Ni nanowires which lead us to obtain important information of the magnetic behavior of the arrays as a function of the length of the nanowires.

## II. EXPERIMENTAL SETUP

Three hexagonal arrays of Ni nanowires of diameters  $d = 2R = 50$  nm and lengths  $L = 1, 4$  and  $12$   $\mu\text{m}$  have been prepared by electrodeposition into nanopores of alumina membranes with interpore distance  $D = 100$  nm [12], [13]. The electrodeposition was performed at a constant potential (dc electrodeposition at  $-1.0$  v). The morphology of the individual nanowires after the dissolution of the alumina was studied by means of scanning electron microscopy (SEM) with a JEOL

5900 LV and transmission electron microscopy (TEM) using a JEOL 2010 F, checking the high ordering of the hexagonal arrays and their large aspect ratio [6].

The chemical characterization of the nanowires was made by means of energy-dispersive analysis of x-rays (EDAX), obtaining a clear peak corresponding to the emission spectrum of Ni. The magnetization measurements were performed with a home-made alternating gradient force magnetometer (AGFM), with the applied field parallel to the axis of nanowires, and at ambient temperature. The samples contain  $\sim 10^9$  Ni nanowires each.

## III. RESULTS AND DISCUSSION

Fig. 1 illustrates the hysteresis curves for the three arrays of nanowires as a function of the length  $L$  of the nanowires. In this figure a strong increase of the coercivity and remanence with the length  $L$  is evidenced. These measurements lead us to obtain the coercivity of the three samples, as illustrated with dots in Fig. 2. In order to understand the dependence of the coercivity on the length, we developed analytical calculations using a simple model. We considered that each nanowire is along the  $z$  axis and reverse its magnetization from one of its minima,  $M = M_0\hat{z}$  to the other,  $M = -M_0\hat{z}$  by means of the propagation of a transversal wall [14]. To calculate the coercivity of an isolated wire we used an adapted Stoner-Wohlfarth model in which the length of the particle which experienced a coherent rotation is replaced by the length of the domain wall. We also included the effect of dipolar interactions of the array, which lowers the energy barriers for the switching. The interaction field was calculated using the expression developed by Laroze *et al.* [15] for the interaction energy of two nanowires a distance  $D$  apart

$$\begin{aligned} \tilde{E}_{\text{int}}(D) &\equiv \frac{E_{\text{int}}(D)}{V} \\ &= \frac{\mu_0 M_0^2 R^2}{2LD} \left( 1 - \frac{1}{\sqrt{1 + \frac{L^2}{D^2}}} \right). \end{aligned}$$

To compare with our experimental results we calculated the non-dimensional magnetostatic interaction energy

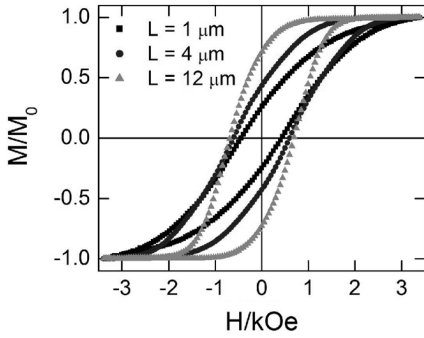


Fig. 1. Hysteresis curves for samples with lengths  $L = 1, 4,$  and  $12 \mu\text{m}$ , inter-pore distance  $D = 100 \text{ nm}$ , and diameter  $d = 2R = 50 \text{ nm}$ , produced under the same chemical conditions. The external magnetic field was applied parallel to the axis of nanowires.

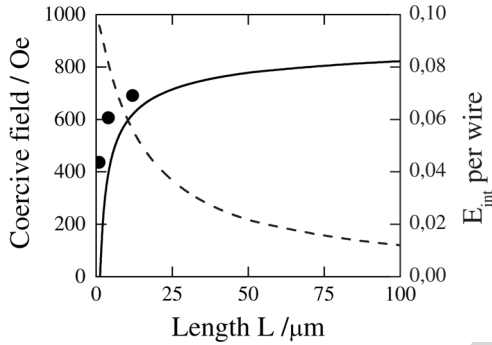


Fig. 2. (Solid line) coercivity calculated for an array of nanowires with  $d = 2R = 50 \text{ nm}$ , and  $D = 100 \text{ nm}$ . (Black dots) experimental values obtained from Fig. 1, and (dash line) the non-dimensional magnetostatic interaction energy per wire as a function of the length  $L$ .

per wire by adding all the contributions in the array,  $\sum_{i=1}^{N-1} \sum_{j=i+1}^N (\dot{E}_{\text{int}}(D)/\mu_0 M_0^2 N)$ , with  $N$  the number of nanowires in the array. Due to present computational capabilities we considered  $N = 70000$ . This energy is illustrated in Fig. 2 with a dashed line. Using these results and following calculations in [6] we obtain the coercivity as a function of the length of the array, which is also depicted with a solid line in Fig. 2. In this figure a good agreement between experimental and analytical results is observed. As a result of the decrease of the interaction energy with the increasing length of the wires in the array, the coercivity decreases approaching the result for the non interacting case ( $E_{\text{int}} = 0$ ). It is also expected a decrease of the interaction field with increasing  $L$  because of the relation between the interaction energy and field.

The measurement of a FORC starts by saturating the sample at a large positive applied field. Then the field is decreased to a reversal field,  $H_a$ . The FORC is defined as the magnetization curve that results when the applied field is increased from  $H_a$  back to saturation. The magnetization at the applied field  $H_b$  on the FORC with reversal point  $H_a$  is denoted by  $M(H_a, H_b)$ , where  $H_b \geq H_a$ .

A statistical model that describes the system as a set of bistable entities (hysteron) based on the Preisach model [7], [16] is used to illustrate and obtain information from the FORC. The

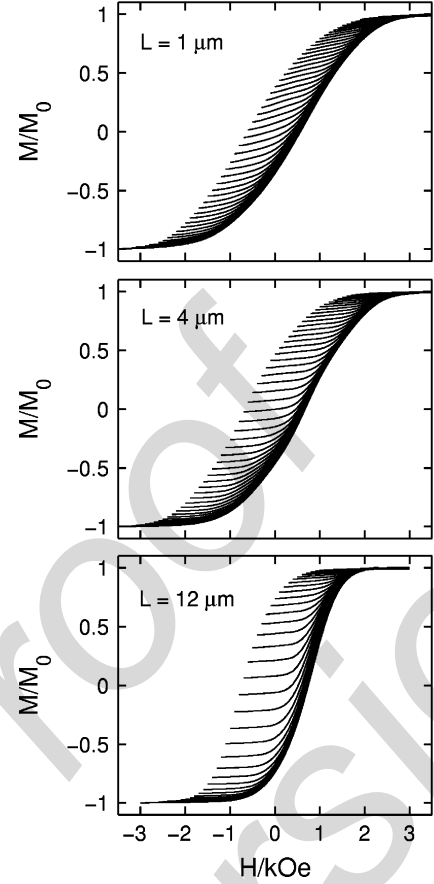


Fig. 3. First order reversal curves (FORC) for samples with different lengths. The external magnetic field was applied parallel to the nanowire axis. Each FORC have been measured with external field intervals of  $100 \text{ Oe}$  between points.

extended probability density function (pdf) of the ensemble is defined by [9], [17]

$$\rho(H_a, H_b) = -\frac{1}{2} \frac{\partial^2 M}{\partial H_a \partial H_b}. \quad (1)$$

This function extends over the entire plane  $H_a, H_b$ . A FORC diagram is a contour plot of the pdf (1), and can be presented in terms of the variables  $H_c = (H_b - H_a)/2$  and  $H_i = (H_b + H_a)/2$  which are the fields of switching (coercivity of hysteron) and interaction (bias of each hysteron) [9], allowing to capture the reversible component of the magnetization, which appears focused on  $H_c = 0$ . The pdf (1) of a sample is obtained by numerical derivation of  $M(H_a, H_b)$ , which contains all FORC measurements. The FORC diagram is obtained performing the contour plot of the pdf (1).

Fig. 3 illustrates the FORCs obtained for the three arrays investigated and Fig. 4 depicts the corresponding contour plots of the pdf (1), i.e., the FORC diagrams of the samples.

In the FORC diagrams of the samples (Fig. 4) a very large distribution of the interaction fields (in the  $H_i$  direction) is observed, which is expected for highly interacting systems. One can also observe from the diagrams that as  $L$  increase the distribution of interaction decrease. This result is in agreement with our analytical results presented in Fig. 2 (dash line) where a

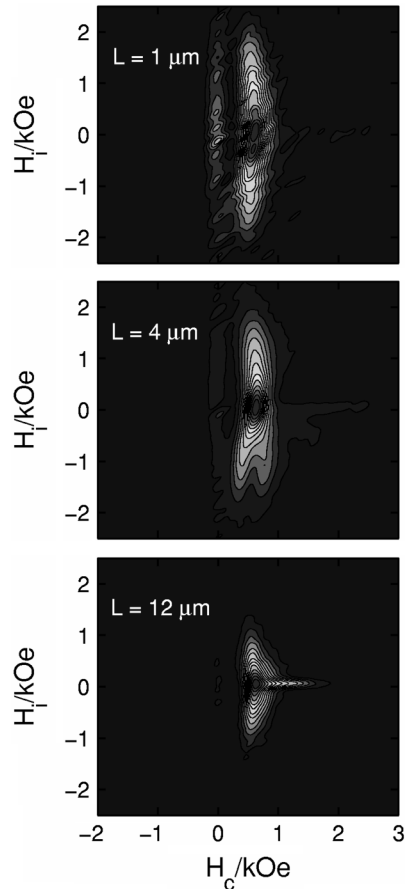


Fig. 4. The FORC diagrams for the three samples studied. These FORC diagrams were obtained performing the contour plots of the pdf (1), and changing to variables  $H_c$  (coercive field) and  $H_i$  (interaction field), according to the text.

strong decrease of the interaction energy by increasing  $L$  is shown. Since the interaction energy is proportional to the interaction field, the decrease of the distribution of the interaction fields when the length of the wires increase, observed in the FORC diagrams, follows the same tendency of the dashed line in Fig. 2.

Fig. 5 depicts the distribution of coercivities at the interaction field  $H_i = 0$ , i.e.,  $\rho(H_c, H_i = 0)/\rho_0$ . In this figure it is shown that by increasing  $L$  the coercivity distribution slightly enhances and the field at which the maximum occur is shifted to higher values. This last feature of the coercivity distribution is in agreement with the behavior of the measured coercivity, which increases for longer nanowires, as shown in Fig. 2. The maximum of the coercive distribution for the three samples are at  $H_c = 574$  Oe,  $H_c = 600$  Oe and  $H_c = 700$  Oe for samples with  $L = 1, 4$ , and  $12 \mu\text{m}$  respectively.

Another important feature which appears in the FORC diagrams is the reversible component of the magnetization. The relative importance of this component, which appears in the FORC diagram at  $H_c = 0$  (Figs. 4 and 5), is not evidenced by measuring the hysteresis curves. This reversible component vanishes as  $L$  increases (Fig. 5), as expected, since a system with

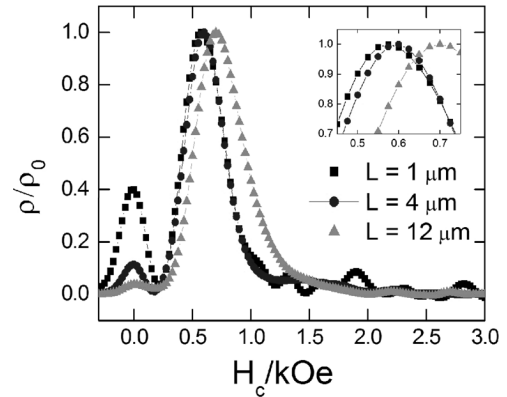


Fig. 5. Distribution of coercivities for the interaction field  $H_i = 0$ , i.e.,  $\rho(H_c, H_i = 0)/\rho_0$ . In the small box it is shown a snapshot of the peaks of the coercivities distribution. At  $H_c = 0$  it is observed a decrease in the reversible component of the magnetization as  $L$  increases.

higher coercivity has a smaller reversible component. Furthermore it is possible to quantify the amount of reversible magnetization of the system as a function of the amount of irreversible magnetization [11], [18].

#### IV. CONCLUSION

The magnetic properties of arrays of Ni nanowires were investigated by means of hysteresis curves and FORC diagrams. Our experimental results were compared with analytical calculations obtained by means of a simple model. The FORC diagrams lead us to obtain a more complete characterization of these systems, giving the coercivity distribution and the reversible and irreversible component of the magnetization, which are difficult to obtain from a simple hysteresis curve. The measured coercivities as a function of the length  $L$  of the wires are in agreement with our analytical results. By increasing the length of the wires in the array an increase of the coercivity and an enhancement of the coercivity distribution are evidenced, as well as a decrease of the reversible component.

#### ACKNOWLEDGMENT

This work was supported in part by the Millennium Science Nucleus *Basic and Applied Magnetism* P06-022F, in part by Fondecyt Grants 11070010, 1080164, and 1080300, and in part by the AFOSR under Contract FA9550-07-1-0040. The CONICYT Ph.D. program and General Direction of Graduates at Universidad de Santiago de Chile (DIGEGRA, USACH) are also acknowledged.

#### REFERENCES

- [1] R. P. Cowburn, D. K. Koltsov, A. O. Adeyeye, M. E. Welland, and D. M. Tricker, "Single-domain circular nanomagnets," *Phys. Rev. Lett.*, vol. 83, pp. 1042–1045, 1999.
- [2] T. Gerrits, H. A. M. van den Berg, J. Hohlfield, L. Bär, and T. Rasing, "Ultrafast precessional magnetization reversal by picosecond magnetic field pulse shaping," *Nature*, vol. 418, pp. 509–512, 2002.

- [3] R. H. Koch, J. G. Deak, D. W. Abraham, P. L. Trouilloud, R. A. Altman, Y. Lu, W. J. Gallagher, R. E. Scheuerlein, K. P. Roche, and S. S. P. Parkin, "Magnetization reversal in micron-sized magnetic thin films," *Phys. Rev. Lett.*, vol. 81, pp. 4512–4515, 1998.
- [4] K. Nielsch, R. B. Wehrspohn, J. Barthel, J. Kirschner, U. Gösele, S. F. Fischer, and H. Kronmüller, "Hexagonally ordered 100 nm period nickel nanowire arrays," *Appl. Phys. Lett.*, vol. 79, pp. 1360–1362, 2001.
- [5] M. Liu, J. Lagdani, H. Imrane, C. Pettiford, J. Lou, S. Yoon, V. G. Harris, C. Vittoria, and N. X. Sun, "Self-assembled magnetic nanowire arrays," *Appl. Phys. Lett.*, vol. 90, no. 103105, 2007.
- [6] J. Escrig, R. Lavín, J. L. Palma, J. C. Denardin, D. Altbir, A. Cortés, and H. Gómez, "Geometry dependence of coercivity in Ni nanowire arrays," *Nanotechnology*, vol. 19, no. 075713, 2008.
- [7] C. R. Pike, A. P. Roberts, and K. L. Verosub, "Characterizing interactions in fine magnetic particle systems using first order reversal curves," *J. Appl. Phys.*, vol. 85, pp. 6660–6667, 1999.
- [8] C. Pike and A. Fernandez, "An investigation of magnetic reversal in submicron-scale Co dots using first order reversal curve diagrams," *J. Appl. Phys.*, vol. 85, pp. 6668–6676, 1999.
- [9] C. R. Pike, "First-order reversal-curve diagrams and reversible magnetization," *Phys. Rev. B*, vol. 68, no. 104424, 2003.
- [10] C. R. Pike, C. A. Ross, R. T. Scalettar, and G. Zimanyi, "First-order reversal curve diagram analysis of a perpendicular nickel nanopillar array," *Phys. Rev. B*, vol. 71, no. 134407, 2005.
- [11] F. Béron, D. Ménard, and A. Yelon, "First-order reversal curve diagrams of magnetic entities with mean interaction field: A physical analysis perspective," *J. Appl. Phys.*, vol. 103, no. 07D908, 2008.
- [12] L. da F. Costa, G. Riveros, H. Gómez, A. Cortés, M. Gilles, E. A. Dalchiele, and R. E. Marotti [Online]. Available: <http://arxiv.org/abs/cond-mat/0504573>
- [13] A. Cortés, G. Riveros, J. L. Palma, J. C. Denardin, R. E. Marotti, E. A. Dalchiele, and H. Gómez, Single-crystal growth of nickel nanowires: influence of deposition conditions on structural and magnetic properties unpublished.
- [14] P. Landeros, S. Allende, J. Escrig, E. Salcedo, D. Altbir, and E. E. Vogel, "Reversal modes in magnetic nanotubes," *Appl. Phys. Lett.*, vol. 90, no. 102501, 2007.
- [15] D. Laroze, J. Escrig, P. Landeros, D. Altbir, M. Vázquez, and P. Vargas, "A detailed analysis of dipolar interactions in arrays of bistable magnetic nanowires," *Nanotechnology*, vol. 18, no. 415708, 2007.
- [16] G. Bertotti, *Hysteresis in Magnetism*. San Diego, CA: Academic Press, 1998.
- [17] L. Spinu, A. Stancu, C. Radu, F. Li, and J. B. Wiley, "Method for magnetic characterization of nanowire structures," *IEEE Trans. Magn.*, vol. 40, pp. 2116–2118, 2004.
- [18] F. Béron, L. Clime, M. Ciureanu, D. Ménard, R. W. Cochrane, and A. Yelon, "Reversible and quasireversible information in first-order reversal curve diagrams," *J. Appl. Phys.*, vol. 101, no. 09J107, 2007.

Manuscript received March 3, 2008. Current version published October 22, 2008. Corresponding author: J. C. Denardin (e-mail: jdenardin@usach.cl).